

## Hydrogen desorption mechanism in MgH<sub>2</sub>-Nb nanocomposites

J. F. Pelletier,<sup>1</sup> J. Huot,<sup>2</sup> M. Sutton,<sup>1</sup> R. Schulz,<sup>2,1</sup> A. R. Sandy,<sup>3</sup> L. B. Lurio,<sup>3</sup> and S. G. J. Mochrie<sup>3</sup>

<sup>1</sup>Centre for the Physics of Materials, McGill University, Montréal, Québec, Canada H3A 2T8

<sup>2</sup>Technologies Émergentes de Production et de Stockage, Institut de Recherche d'Hydro-Québec, Varennes, Québec, Canada J3X 1S1

<sup>3</sup>Center for Materials Science and Engineering, Massachusetts Institute of Technology, Cambridge, Massachusetts 02139-4307

(Received 23 October 2000; published 12 January 2001)

*In situ* time-resolved x-ray scattering measurements of hydrogen desorption in MgH<sub>2</sub>-Nb nanocomposites using synchrotron radiation are presented. Results show that niobium acts like a catalyst for hydrogen absorption and desorption. It is found that hydrogen desorption involves the formation of a short-lived metastable niobium-hydride phase which acts as a gateway through which hydrogen released from MgH<sub>2</sub> is flowing. The desorption kinetics of this system is revealed through temporal profiles showing the lifetimes of the different phases involved.

DOI: 10.1103/PhysRevB.63.052103

PACS number(s): 61.46.+w, 61.10.-i, 64.60.My, 84.60.Ve

The growing concern about air pollution and the greenhouse effect has promoted the development of nonpolluting energy sources in the past 30 years. In the particular case of automotive fuel, hydrogen has been proposed for use with both internal combustion engines and fuel cells. For either case, a safe and efficient way of storing and transporting hydrogen has to be developed. Metal hydrides are a promising solution to the storage problem for hydrogen-energy applications since they store hydrogen at low pressure yet have volumetric densities comparable to liquid hydrogen.<sup>1</sup> Another advantage is the fact that hydrogen is released through an endothermic process making hydrogen storage in metal hydrides inherently safe. Magnesium hydride is a particularly interesting prospect due to its high storage capacity per unit weight but one of its disadvantages is slow hydrogen sorption kinetics. However several recent developments involving nanocrystalline metal hydrides have greatly contributed to the solution of this limitation.<sup>2</sup>

First, it has been shown that nanocrystalline magnesium hydride formed by energetic ball milling of MgH<sub>2</sub> have much improved sorption kinetics over conventional polycrystalline MgH<sub>2</sub>.<sup>3</sup> This improved kinetics is due to the high density of defects and grain boundaries in the nanocrystalline material. An added advantage is the ease of synthesis that is especially important for magnesium-based alloys given magnesium's low melting point. A second improvement is the use of metal additives which act as catalysts or facilitators to further enhance the sorption kinetics of hydrogen in magnesium hydrides.<sup>4</sup> These additives are easy to incorporate by ball milling and examples include Pd, Ni, Ti, Fe, LaNi<sub>5</sub>, V as well as many others. Of these metals that form a low-temperature hydride, vanadium shows great potential. In addition to being relatively light, adding 5 at. % of vanadium improves sorption times by an order of magnitude at 300 °C.<sup>5</sup> Vanadium and magnesium are immiscible and milling MgH<sub>2</sub> with V forms a mixture of MgH<sub>2</sub>-VH<sub>x</sub> and it appears that VH<sub>x</sub> acts as the facilitator for hydrogen adsorption and desorption.

Although empirical studies have shown that the addition of a low-temperature hydride (i.e., hydride that can reversibly absorb hydrogen at temperatures lower than 80 °C) enhances the hydrogen sorption kinetics, the exact role of the

additive and the mechanism by which hydrogen flows in and out of the hydride still remain unclear. In order to have a better understanding of this mechanism, we have used *in situ* time-resolved x-ray scattering to probe the structure evolution of MgH<sub>2</sub>-5 at. % Nb nanocomposites during hydrogen desorption. Niobium was used instead of vanadium since it is a better x-ray scatterer and the sorption properties of this system are similar to those of MgH<sub>2</sub>-5 at. % V.<sup>6</sup> Although numerous x-ray-diffraction investigations have been reported,<sup>7</sup> here we use *in situ* time-resolved x-ray scattering to study structural changes during hydrogen desorption. Our analysis reveals that for MgH<sub>2</sub>-5 at. % Nb, hydrogen desorption involves the formation of an intermediate niobium-hydride phase which appears to be the key element responsible for the improved desorption kinetics of this nanocomposite. Our results also show the catalyticlike process involved in this system.

A composition of MgH<sub>2</sub>-5 at. % Nb made from a mixture of pure magnesium hydride and niobium powder was mechanically milled in a Spex 8000 shaker mill under argon atmosphere during 20 h as described in Ref. 5. The resulting nanocomposite powder was cold pressed into a 1-mm-thick pellet under a pressure of 1 GPa for 2 min. The measurements were performed using a spectrometer optimized for time resolved x-ray diffraction<sup>8</sup> on the MIT-McGill-IBM beamline at the Advanced Photon Source. A diamond crystal monochromator is used to produce 7.66-keV x rays having a relative bandwidth  $\Delta\lambda/\lambda = 6.2 \times 10^{-5}$  and a flux of  $\sim 5 \times 10^{12}$  photons per second for a storage ring current of 100 mA. Scattered x rays were collected by a linear photodiode array detector (PSD).<sup>9</sup> The detector was located 75 mm from the sample covering a range of 20° in  $2\theta$ . Scattering patterns could be acquired every 5 ms. Samples were loaded inside a vacuum furnace with a Be window permitting access to approximately 200° in  $2\theta$ . The furnace was pumped down to a base pressure of  $\sim 1 \times 10^{-6}$  Torr prior to heating the sample.

X-ray powder-diffraction spectra of the hydrided and dehydrided state of MgH<sub>2</sub>-Nb are shown in Figs. 1(a) and 1(b), respectively. Figure 1(a) shows the structure of the hydrided sample as synthesized. As a result of the ball-milling process, the metastable  $\gamma$ -MgH<sub>2</sub> phase is synthesized<sup>3</sup> as well as the  $\beta$ -NbH phase. A small amount of magnesium oxide is

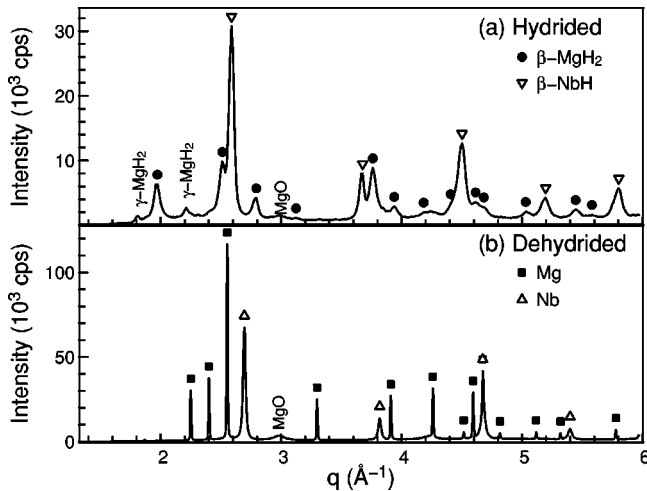


FIG. 1. Powder-diffraction patterns of  $\text{MgH}_2\text{-Nb}$ : (a) hydrided and (b) dehydrided after annealing at  $310^\circ\text{C}$  for 1500 sec in vacuum. Intensities are normalized to a storage-beam current of 100 mA.

present in the as ball-milled powder. Figure 1(b) shows a typical dehydrided spectrum obtained after annealing at  $310^\circ\text{C}$  for 1500 s in vacuum. Both magnesium and niobium have totally released their hydrogen and only metallic phases are present. Total dehydrogenation of niobium hydride was possible since the pressure inside the sample chamber was much smaller than the equilibrium pressure of  $\beta\text{-NbH}$ , as indicated in the pressure-composition-temperature curves given in Ref. 10. There is also a slight increase of magnesium oxide compared to the as ball-milled state. As seen in Fig. 1, the different lattice constants in the  $\text{MgH}_2\text{-Nb}$  system provides diffraction patterns for the initial and final stages with many nonoverlapping peaks so each phase can easily be identified.

A typical time-resolved x-ray scattering data set is presented in Fig. 2. Figure 2(a) shows a gray-scale contour plot of the x-ray scattering intensity while the sample was being heated and Fig. 2(b) shows the sample temperature as a function of time. The different peaks corresponding to the start and end product are labeled on the right-hand side of the graph. Dehydrogenation of magnesium hydride starts at  $\sim 370$  s, when temperature has reached  $\sim 275^\circ\text{C}$ , and is completed in less than 100 s. The first striking feature of this data set is the observation of niobium hydride forming a short-lived metastable phase which is maintained for approximately 200 s before finally desorbing into metallic Nb. The current setup only allowed for relatively slow cooling rates ( $\sim 20^\circ\text{C}/\text{min}$ ) and attempts to quench the metastable phase to further study its nature have remained unsuccessful. The second striking feature from this measurement is the fact that the intensity of the  $\beta\text{-MgH}_2$  peaks increases with temperature until the onset of desorption at  $\sim 370$  s. Finally, looking at this image closely also reveals that the  $\beta\text{-MgH}_2$  peaks are slightly moving toward smaller  $q$  as temperature increases, indicating a small change of lattice parameters due to thermal expansion.

The time evolution of the different magnesium and niobium phases is presented in Fig. 3(a). Reliable volume frac-

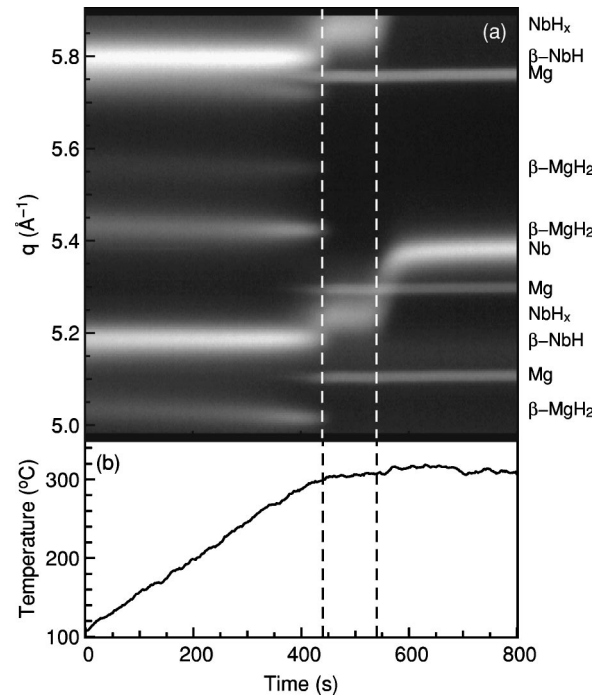


FIG. 2. Time-resolved x-ray scattering data for  $\text{MgH}_2\text{-Nb}$  heated to  $310^\circ\text{C}$ . (a) Gray-scale contour plot of the x-ray scattering where intensity increases with lighter tones, (b) temperature profile. The dashed lines are intended as a visual aid and indicate the time interval where a metastable phase exists.

tions for each of these phases were obtained by decomposing the total diffraction pattern into the sum of diffraction patterns for each phase.<sup>11</sup> As the temperature increases from  $170^\circ\text{C}$  to about  $270^\circ\text{C}$ , there is no indication of the formation of metallic magnesium. Even though no dehydrogenation occurs, we observe that the  $\beta\text{-MgH}_2$  phase grows at the same rate as the metastable  $\gamma\text{-MgH}_2$  phase is being depleted. This is a direct confirmation that the metastable  $\gamma\text{-MgH}_2$  phase indeed transforms into  $\beta\text{-MgH}_2$  before the onset of hydrogen desorption as has been found from DTA measurements.<sup>12</sup> In the present case, the transformation appears at a much lower temperature ( $170^\circ\text{C}$  instead of  $325^\circ\text{C}$  in Ref. 12) due to the nanocrystalline nature of the materials involved. Dehydrogenation of magnesium hydride starts at around  $275^\circ\text{C}$  and is reflected by a linear trade-off between the increase in metallic magnesium and the decrease of the  $\beta\text{-MgH}_2$  peaks.

From Figs. 2(a) and 3(a) it can be seen that there is not a single transition from  $\beta\text{-NbH}$  to metallic niobium and it is evident that all the initial  $\beta\text{-NbH}$  phase transforms into a temporary metastable phase, that we shall refer to as  $\text{NbH}_x$ . Figure 3(a) distinctively shows that the metastable phase appears simultaneously with metallic magnesium.  $\text{NbH}_x$  reaches its maximum at  $t=475$  s exactly at the same time as  $\beta\text{-MgH}_2$  disappears and Mg has completely formed. It is only when the hydrogen flow from  $\beta\text{-MgH}_2$  has stopped that  $\text{NbH}_x$  starts transforming into metallic Nb. Peaks of the metastable phase have been observed at  $q=3.703, 4.543, 5.240,$  and  $5.861 \text{ \AA}^{-1}$  but we were not able to identify it to any known niobium hydride phase described in the literature.

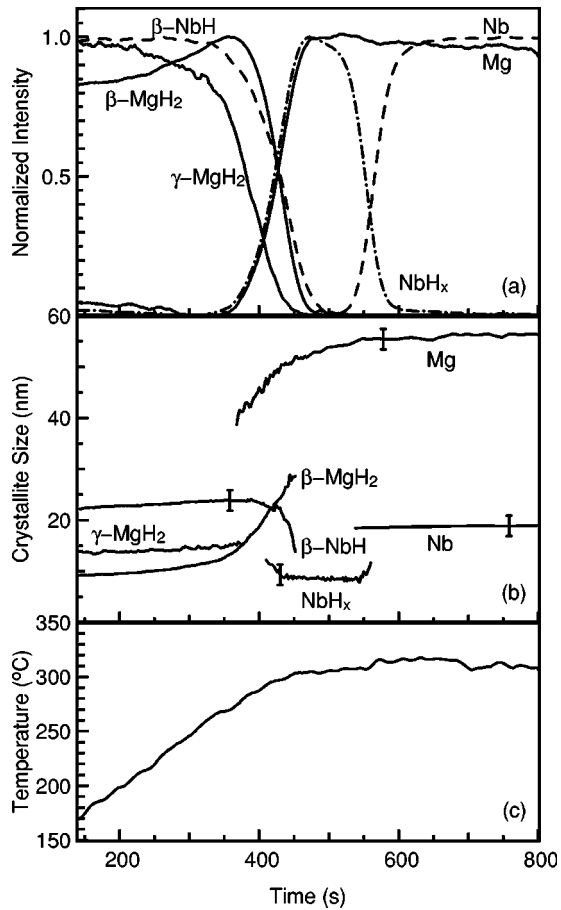


FIG. 3. Temporal evolution of: (a) the relative normalized intensity, (b) crystallite sizes for the different hydride and metallic phases of magnesium and niobium, and (c) sample temperature.

However, it has been shown that lattice parameters of niobium hydride change linearly with hydrogen concentration at temperatures above  $\sim 160^\circ\text{C}$ .<sup>13,10</sup> Using the relation between unit-cell volume change and hydrogen concentration in NbH<sub>x</sub>,<sup>13</sup> we estimated that the metastable NbH<sub>x</sub> phase corresponds to a hydrogen content of NbH<sub>0.6</sub>. This concentration is close to the  $\varepsilon$  phase (Nb<sub>4</sub>H<sub>3</sub>). However, from the phase diagram,<sup>10</sup> one would not expect to observe the  $\varepsilon$  phase in our experimental conditions since it is only stable at temperatures below  $-48^\circ\text{C}$ . On the other hand, Fig. 3(a) clearly shows that the intensity of the metastable niobium phase increases simultaneously with the intensity of metallic magnesium and only after the magnesium is fully dehydrided, does the metastable phase transform into niobium. In addition to the well-known effect of metal for dissociating H<sub>2</sub> into atomic hydrogen, we propose that niobium in Mg-Nb acts as a gateway through which hydrogen flows to get out of the magnesium matrix.<sup>14</sup> This is in contrast to the spillover model<sup>15</sup> which would have surface diffusion controlling the hydrogen uptake in Mg.

Metallic Nb does not appear until the  $\beta$ -MgH<sub>2</sub> has completely desorbed, implying that the metastable niobium phase does not spontaneously decay into Nb. Thus it appears that the NbH<sub>x</sub> phase is stabilized by the hydrogen flow. Considering this, and the fact that the temperature is constant during

the metastable phase decay, a possible explanation for the appearance of the metastable phase could be that the hydrogen released from magnesium hydride is passing through niobium hydride where it forces the hydrogen atoms to assume specific locations in the NbH lattice in order to facilitate the hydrogen flow. This would produce a long-range order of hydrogen atoms in the niobium structure before total dehydrogenation which seems to be closely related to the  $\varepsilon$ -NbH phase. The  $\varepsilon$  phase is an ordering of vacancies on a hydrogen sublattice of the  $\beta$  phase.<sup>10</sup> Ordering of the  $\alpha$ ,  $\alpha'$  phase of NbH has been observed at several hundred degrees above  $T_c$ .<sup>16</sup> Further evidence is that the diffusion coefficient of hydrogen in Nb reaches a maximum for a concentration H/Nb  $\approx 0.6$ ,<sup>17</sup> which corresponds to the value inferred for the metastable niobium hydride phase. Experiments at 250, 280, and 310  $^\circ\text{C}$  indicated that the kinetics of the metastable phase formation and decomposition are temperature dependent. From an Arrhenius plot, the activation energy of formation of metastable niobium hydride was found to be  $65 \pm 2$  kJ/mol. This value is very close to the activation energy of 62 kJ/mol deduced from hydrogen desorption kinetic of magnesium hydride in the similar Mg-V system.<sup>5</sup>

A simple volume fraction model, would suggest a nucleation and growth process which might be initiated by the nucleation of NbH<sub>x</sub> and Mg at the interface of  $\beta$ -NbH and  $\beta$ -MgH<sub>2</sub>. Based on the gateway model we are proposing, one should expect the volume fraction of Mg and NbH<sub>x</sub> to track at the start of the transformation. However, it is not clear how such a model would explain why these phases reach completion at the same time as shown in Fig. 3(a). If not enough  $\beta$ -NbH was available to react, one would expect a measurable volume fraction of  $\beta$ -MgH<sub>2</sub> to remain, similarly, for an excess one would expect  $\beta$ -NbH to remain. The amount of niobium additive used in this experiment (5 at. %) was optimized to obtain the fastest hydrogen release for the smallest amount of niobium. In the context of the gateway model, this optimization could explain why the volume fractions track.

Finally, it is evident from Fig. 1 that magnesium undergoes grain growth. We were able to measure this grain growth *in situ* as shown in Fig. 3(b) where the crystallite size of the different phases is plotted against time. The crystallite size was evaluated using Scherrer's method. In the initial stage, crystallite size of the  $\gamma$ -MgH<sub>2</sub> phase remains at  $\sim 15$  nm while it transforms into  $\beta$ -MgH<sub>2</sub>. This transformation causes a coherent growth of the  $\beta$  phase whose size increases from 9 to 15 nm. During that same period,  $\beta$ -NbH crystallite size barely increases from 22 to 24 nm. Once dehydrogenation begins at  $\sim 370$  s, we observe a sharp increase in the size of  $\beta$ -MgH<sub>2</sub> crystallites from 15 to 30 nm while  $\beta$ -NbH decrease rapidly from 24 to 14 nm. The size of  $\beta$ -NbH decrease is consistent with its volume fraction reduction. The NbH<sub>x</sub> phase displays a small crystallite size of about 8–10 nm comparable to the initial size of  $\beta$ -MgH<sub>2</sub> which is consistent with the proposed gateway model. During the desorption process metallic Mg particles appear and undergo growth from 40 to 55 nm. At  $\sim 550$  s, once dehydrogenation has completed, the width of the peaks from the

metallic Mg and Nb phases remains constant with particle sizes of the order of 57 and 20 nm, respectively.

Using time-resolved x-ray scattering, we have found that an intermediate niobium hydride phase forms during hydrogen desorption with an approximate composition of  $\text{NbH}_{0.6}$ . We propose a model in which the niobium nanoparticles act as gateway for hydrogen flowing out of the magnesium reservoir. Explanations of heterogenous catalytic reaction such as the spillover effect and gateway models have been proposed over the years. This is direct evidence of the hydroge-

nation mechanism in such composite metal hydrides. This gateway mechanism might also play a role in other cases of heterogenous catalysis.

Beamline 8-ID was developed with support from the NSF Instrumentation for Materials Research Program (DMR 9312543), from the DOE Facilities Initiative Program (DE-FG02-96ER45593), and from NSERC. Use of the Advanced Photon Source was supported by the U.S. Department of Energy, Basic Energy Sciences, Office of Science, under Contract No. W-31-109-Eng-38.

- 
- <sup>1</sup>D.L. Douglass, in *Hydrides for Energy Storage*, edited by A.F. Andresen and A.J. Maeland (Pergamon, Geilo, Norway, 1977), p. 151; J.J. Reilly, *Z. Phys. Chem., Neue Folge* **117**, 155 (1979); P. Hoffmann, *The Forever Fuel* (Westview Press, Boulder, CO, 1981).
- <sup>2</sup>L. Zaluski, A. Zaluska, P. Tessier, J.O. Ström-Olsen, and R. Schulz, *Mater. Sci. Forum* **225-227**, 853 (1996); S. Orimo and H. Fujii, *Intermetallics* **6**, 185 (1998).
- <sup>3</sup>J. Huot, G. Liang, S. Boily, A. van Neste, and R. Schulz, *J. Alloys Compd.* **293-295**, 495 (1999).
- <sup>4</sup>L. Zaluski, A. Zaluska, and J.O. Ström-Olsen, *J. Alloys Compd.* **253-254**, 70 (1997); G. Liang, J. Huot, S. Boily, A. van Neste, and R. Schulz, *ibid.* **292**, 247 (1999).
- <sup>5</sup>G. Liang, J. Huot, S. Boily, A. van Neste, and R. Schulz, *J. Alloys Compd.* **291**, 295 (1999).
- <sup>6</sup>R. Schulz *et al.*, International Patent Application No. PCT/Ca98/00987 (1997).
- <sup>7</sup>Z. Gavra and J.J. Murray, *Rev. Sci. Instrum.* **57**, 1590 (1986); K.J. Gross, S. Guthrie, S. Takara, and G. Thomas, *J. Alloys Compd.* **297**, 270 (2000).
- <sup>8</sup>J.F. Pelletier *et al.* in *Synchrotron Radiation Instrumentation*, AIP Conf. Proc. No. **521** (AIP, Melville, NY, 2000), p. 188.
- <sup>9</sup>G.B. Stephenson, *Nucl. Instrum. Methods Phys. Res. A* **266**, 447 (1988).
- <sup>10</sup>T. Schober, in *Hydrogen Metal Systems I*, edited by F.A. Lewis and A. Aladjem (Trans Tech Publications, Ltd, Zurich, 1996), p. 357.
- <sup>11</sup>See Appendix of S. Brauer *et al.*, *Phys. Rev. B* **45**, 7704 (1992).
- <sup>12</sup>J.-P. Bastide, B. Bonnetot, J.-M. Letoffe, and P. Claudy, *Mater. Res. Bull.* **15**, 1215 (1980).
- <sup>13</sup>M.A. Pick and R. Bausch, *J. Phys. F: Met. Phys.* **6**, 1751 (1976).
- <sup>14</sup>A similar gateway model was proposed for the catalytic role of  $\text{Mg}_2\text{Cu}$  in the eutectic alloy Mg/ $\text{Mg}_2\text{Cu}$  by J. Genossar and P.S. Rudman, *Z. Phys. Chem., Neue Folge* **116**, 215 (1979).
- <sup>15</sup>W. Curtis Conner and J.L. Falconer, *Chem. Rev.* **95**, 759 (1995).
- <sup>16</sup>E. Burkel, H. Behr, H. Metzger, and J. Peisl, *Phys. Rev. Lett.* **46**, 1078 (1981).
- <sup>17</sup>Y. Fukai, *The Metal-Hydrogen System* (Springer-Verlag, Berlin, 1993), p. 248.